

| | $t \rightarrow \infty$ | $t \nrightarrow \infty$ |
|-------------------------|--|---|
| $C \rightarrow \infty$ | $\eta_{\max} = \eta_C$ | $\frac{\eta_C}{2} \leq \eta_{\text{EMP}} \leq \frac{\eta_C}{2-\eta_C}$ |
| $C \nrightarrow \infty$ | $1 + \frac{(1-\eta_C) \ln(1-\eta_C)}{\eta_C} \leq \eta_{\text{EMW}} \leq 1 + \frac{\eta_C}{\ln(1-\eta_C)}$ | $1 + \frac{\eta_C/2}{\ln(1-\eta_C/2)} \leq \eta^{\text{FT}} \leq 1 + \frac{1-\eta_C}{\eta_C/2} \ln \frac{1-\eta_C}{1-\eta_C/2}$ |

Table I. Bound for efficiency in different case. Here t is the operation time of the heat engine and C is the heat capacity of the heat source. In the case engine working in quasi-static cycle between infinite heat bath, i.e., $t \rightarrow \infty, C \rightarrow \infty$, the maximum achievable efficiency, as stated by Carnot, is the Carnot efficiency $\eta_C = 1 - T_L/T_H$. For the engine operates in finite time, i.e., $C \rightarrow \infty, t \nrightarrow \infty$, Esposito et al. [38] give the bounds for the efficiency at maximum power (EMP) with low-dissipation Carnot-like engine. We show the bounds for efficiency at maximum work (EMW) ($t \rightarrow \infty, C \nrightarrow \infty$) and efficiency at maximum power for each cycle ($t \nrightarrow \infty, C \nrightarrow \infty$) obtained in this paper. The detailed derivations are illustrated in Sec. II A and Sec. III respectively. The bounds in the latter two cases for η_{EMW} and η^{FT} in this table are limited to the heat source having a positive and constant heat capacity. The bounds correspond to heat capacity change with temperature are discussed in Sec. II B while the negative heat capacity case are discussed in Sec. IV.

Effect of finite-size heat source's heat capacity on the efficiency of heat engine

Yu-Han Ma^{1,2,*}

¹*Beijing Computational Science Research Center, Beijing 100193, China*

²*Graduate School of China Academy of Engineering Physics,
No. 10 Xibeiwang East Road, Haidian District, Beijing, 100193, China*

Heat engines used to output useful work have important practical significance, which, in general, operate between heat baths of infinite size and constant temperature. In this paper we study the efficiency of a heat engine operating between two finite-size heat sources with initial temperature differences. The total output work of such heat engine is limited due to the finite heat capacity of the sources. We investigate the effects of different heat capacity characteristics of the sources on the heat engine's efficiency at maximum work (EMW) in the quasi-static limit. In addition, we study the efficiency of the engine working in finite-time with maximum power of each cycle is achieved and find the efficiency follows a simple universality as $\eta = \eta_C/4 + O(\eta_C^2)$. Remarkably, when the heat capacity of the heat source is negative, such as the black holes, we show that the heat engine efficiency during the operation can surpass the Carnot efficiency determined by the initial temperature of the heat sources. It is further argued that the heat engine between two black holes with vanishing initial temperature difference can be driven by the energy fluctuation. The corresponding EMW is proved to be $\eta_{\text{EMW}} = 2 - \sqrt{2}$, which is two time of the maximum energy release rate $\mu = (2 - \sqrt{2})/2 \approx 0.29$ of two black hole emerging process obtained by S. W. Hawking.

I. INTRODUCTION

As one of the most useful devices in modern society, the heat engine converts the heat extracted from the heat source into useful work, which is one of the core fields in thermodynamic research [1–8]. Early heat engine research was limited to reversible cycles in the quasi-static limit, with which, as stated by the Carnot's theorem [1], the achievable maximum efficiency of heat engines is the so-called Carnot efficiency $\eta_C = 1 - T_L/T_H$, where T_H (T_L) is the temperature of the hot (cold) bath. Since the last century, with the maturity of quantum theory and its related technologies, people started to pay attention to the performance of quantum heat engines working in micro-scale within the framework of quan-

tum thermodynamics[3, 4, 7–18]. Series of the quantum effect, such as coherence, entanglement, quantum phase transition, etc., of the working substance or heat source have been studied to realize better heat engines [12, 19–26]. On the other hand, with the development of non-equilibrium thermodynamics[2, 27], the optimization of actual heat engines under the framework of finite-time thermodynamics attracted a wide range of attention [28–32]. Extensive research on the efficiency at maximum power (EMP) [33–39], trade-off relation between power and efficiency [40–43], and optimal operation of heat engine have been proposed [44, 45]. The motivation for these studies stems from the fact that time is a finite resource, we cannot trade at the cost of infinitely long working time for heat engines that are efficient but have vanishing output power.

* yhma@csrc.ac.cn

Most of studies about heat engines have regarded the thermal source as an infinite system, that is, it can continuously provide heat. However, just like time, the heat source is also a finite resource, so it is an interesting and practical task to consider the optimization of the heat engine working between finite-size heat sources. Recently, people began to consider this issue with different perspectives. For example, considering the Carnot heat engine working between finite heat sources [46–48], linear irreversible heat engines working in finite time with finite-size bath [49, 50], and the bounds of optimal efficiency the engines can achieve [51, 52]. In addition, the influences of the finite-size heat source on the quantum heat engine [53–57] and quantum battery [58] also attract some attention. In general, the finite-size effect of the heat source is reflected in the limited heat capacity. Therefore, the nature of the heat capacity of the heat sources directly determines the performance of the heat engine working between them. In this paper, we discuss the effects of finite-size heat sources with different heat capacity characteristics on heat engine’s efficiency, in both quasi-static and finite-time circumstances. We obtain some bounds for the efficiency and list them in Tab. I. In particular, we study the case where the heat source has a negative heat capacity, which is proved to be advantageous for improving the efficiency of the heat engine. To our best knowledge, this has never been reported before.

The paper is organized as follows: In Sec. II, we first generally discuss the influence of the heat capacity of the finite-size heat sources on the efficiency of the heat engine at maximum work (EMW) with quasi-static cycle. Then the efficiency of the heat engine in the high and low temperature limit with different heat capacity function are derived. In the low-temperature regime, it is found that the dimension of the heat source will influence the EMW of the heat engine, and the higher EMW can be achieved with higher dimension materials. In Sec. III, the study in quasi-static situation is extend to the finite-time case, where we consider the low-dissipation Carnot-like heat engine working between two finite-size sources. We point out that when the heat engines operates with maximum power in each cycle, the efficiency of the whole process follows a simple universality as $\eta = \eta_C/4 + O(\eta_C^2)$. With the black hole as an illustration, we study the negative heat capacity system service as the finite-size heat source in Sec. IV. Conclusion and discussions are given in Sec. V.

II. HEAT ENGINE WORKING BETWEEN FINITE-SIZE HEAT SOURCE

As shown in Fig. 1, we consider the heat engine of interest is working between two heat source H and L with finite size, where T_H (T_L) and C_H (C_L) are the initial tem-

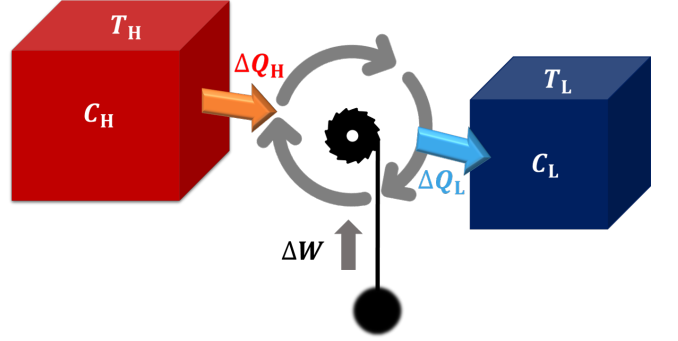


Figure 1. Heat engine working between two finite-size heat sources. T_H (T_L) and C_H (C_L) are the initial temperature and heat capacity of the high (low) temperature source H (L) respectively. $\Delta W = \sum_{\alpha=H,L} \Delta Q_\alpha$ is the output work of the engine per cycle while ΔQ_H is the heat absorbed from the hot source and ΔQ_L the heat releases to the cold source.

perature and heat capacity of the high (low) temperature source H (L) respectively. With the working substance S run through an arbitrary thermodynamic cycle, the heat engine can generate output work $\Delta W = \int_0^\tau dW$ per cycle. Here τ is the cycle time, and $\Delta W = \sum_{\alpha=H,L} \Delta Q_\alpha$, $\Delta Q_H = -\int_0^\tau dQ_H$ is the heat absorbed from the high temperature source and $\Delta Q_L = \int_0^\tau dQ_L$ the heat releases to the low temperature heat source. When the heat engine works after many cycles, we can evaluate the heat engine’s performance with its efficiency η and power P , namely,

$$\eta = \frac{\int_0^t dW}{-\int_0^t dQ_H}, P = \frac{\int_0^t dW}{t} \quad (1)$$

where t is the engine’s total working time. For the size of these two heat sources approach infinite as well as the heat capacity, i.e., $C_{H,L} \rightarrow \infty$, their temperature will remain constant as the initial time. In such case, the two heat sources service as two heat bath, and the maximum efficiency of the heat engine is bounded by the well-known Carnot efficiency

$$\eta_C = 1 - \frac{T_L}{T_H}, \quad (2)$$

which can be achieved when the working substance works under a reversible Carnot cycle with vanishing output power. However, for the heat sources with finite size, their temperature will change as the heat engine works. Specifically, after providing heat to the working substance, T_H of the high-temperature heat source decreases. And on the other hand, the low-temperature source’s

temperature T_L increases since the working substance releases heat to it. Here we have assumed $C_{H,L} > 0$ since most physical systems have positive heat capacity, and the extreme special situation where the heat sources have negative heat capacity i.e., $C_{H,L} < 0$ will be discussed in Sec. IV. As the time goes by, the heat engine will finally stop outputting work when the temperature of the two heat sources become the same, namely, $T_H(t_f) = T_L(t_f)$, where t_f is introduced as the stop time of the heat engine. The corresponding efficiency

$$\eta(t_f) = \frac{\int_0^{t_f} dW}{-\int_0^{t_f} dQ_H} \quad (3)$$

is called the efficiency at maximum work (EMW) [49, 59] and we denote it as $\eta(t_f) \equiv \eta_{\text{EMW}}$ thereafter. Generally, the temperature change of the source per cycle is $\Delta T_\alpha = \Delta Q_\alpha / C_\alpha$ ($\alpha = H, L$) with $\Delta Q_\alpha \propto C_S (T_H - T_L)$, thus the stop time t_f depends on the ratio of the heat capacity of the sources and working substance as $t_f \propto \min\{C_H, C_L\} / C_S \tau$. When the heat source and the working substance are about the same size ($C_S \sim C_H$), the heat engine can only work for a few cycles or even less than one cycle, and the heat engine in such circumstance does not have practical use value. In the following discussion, we focus on the situation that the heat engine can work with limited but sufficient cycles, i.e., $t_f / \tau \gg 1$ with $C_S / C_\alpha \ll 1$.

With the work of the heat engine keeps going on, noticing the temperature difference of the two source become smaller and smaller, thus we have [49]

$$\eta_{\text{EMW}} = 1 + \frac{\int_0^{t_f} dQ_L}{\int_0^{t_f} dQ_H} < 1 + \frac{\int_0^{t_f} T_L dS_L}{\int_0^{t_f} T_H dS_H} \leq \eta_C, \quad (4)$$

where the equal sign on the right side only hold in the reversible limit with $\int_0^{t_f} dS_L = -\int_0^{t_f} dS_H$. The above discussion implies that it is the finite heat capacity of the heat sources limit the EMP the heat engine can achieve. Therefore, the following two questions naturally raises: (i) What's the heat engine's maximum EMP when working at two finite-size heat bath. (ii) How the specific feature of the heat source's heat capacity affects such EMP. We first rewrite the efficiency of Eq. (4) in term of C_H and C_L as

$$\eta_{\text{EMW}} = 1 + \frac{\int_0^{t_f} C_L dT_L}{\int_0^{t_f} C_H dT_H}, \quad (5)$$

where $\int_0^{t_f} dQ_\alpha = \int_0^{t_f} dU_\alpha = \int_0^{t_f} C_\alpha dT_\alpha$ ($\alpha = H, L$) have been used for the two heat sources. For a given physical system, heat capacity is generally the function of temperature, i.e., $C_{H,L} = C_{H,L}(T)$, and one can complete the integral in Eq. (5) explicitly with the specific form of

$C_{H,L}(T)$. Assuming the heat capacity of the sources follow the Debye's Law [60], for example most of the crystal, thus $C(T) = \text{const}$ in the high temperature regime of $T/\Theta \gg 1$, and $C(T) \propto T^n$ in the low-temperature regime of $T/\Theta \ll 1$. Here Θ and n are the Debye temperature and the dimension of material respectively.

A. High temperature regime

In this case, the heat capacity only determined by the size (particle number) of the source, such that Eq. (5) is simplified as

$$\eta_{\text{EMW}} = 1 - \frac{C_L [T_L(t_f) - T_L]}{C_H [T_H - T_H(t_f)]}, \quad (6)$$

where $T_L(t_f) = T_H(t_f) \equiv T_E$ is the equilibrium temperature of the two sources. The EMW is achieved with the reversible cycle, in which no irreversible entropy is generated, i.e., $\sum_{\alpha=H,L,S} \int_0^{t_f} S_\alpha = 0$. Noticing $C_S / C_\alpha \ll 1$, the entropy change of the working substance $\int_0^{t_f} S_S$ can be ignored, then we have

$$\int_0^{t_f} \left(\frac{dQ_H}{T_H} + \frac{dQ_C}{T_C} \right) = 0, \quad (7)$$

which is further written as

$$\int_0^\tau \frac{C_L dT_L}{T_L} + \int_0^\tau \frac{C_H dT_H}{T_H} = 0 \quad (8)$$

This is the reversible condition of the whole process. Finish the integral in Eq. (8), we find the equilibrium temperature

$$T_E = T_H (1 - \eta_C)^{\frac{\xi}{\xi+1}}, \quad (9)$$

where $\xi \equiv C_L / C_H$ is defined as the heat capacity ratio between the low and high temperature heat source. ξ characterizes the asymmetry of two heat sources. By substituting Eq. (9) into Eq. (6), the EMW is obtained in terms of ξ and η_C as

$$\eta_{\text{EMW}} = 1 - \frac{\xi \left[(1 - \eta_C)^{\frac{\xi}{\xi+1}} - (1 - \eta_C) \right]}{1 - (1 - \eta_C)^{\frac{\xi}{\xi+1}}}. \quad (10)$$

Here $\eta_C = 1 - T_L / T_H$ is the Carnot efficiency determined by the initial temperature of the sources. We illustrated η_{max} as the function of η_C in Fig. 2. In three different limit case, namely, the symmetry case of $\xi = 1$, infinite low-temperature source size of $\xi \rightarrow \infty$, and infinite high-temperature source size of $\xi \rightarrow 0$, we simplify Eq. (10) as follows

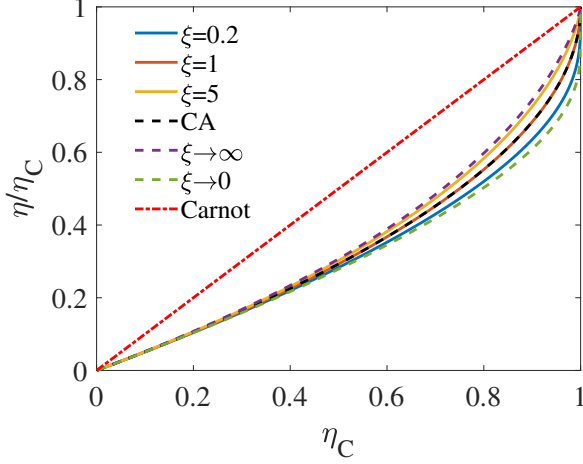


Figure 2. EMW η_{EMW} as the function of η_C with different $\xi = C_L/C_H$. The curve relates to infinite low-temperature source size ($\xi \rightarrow \infty$) and infinite high-temperature source size ($\xi \rightarrow 0$) are given by Eq. (11). The other are plot with Eq. (10).

$$\eta_{\text{EMW}} = \begin{cases} 1 - \sqrt{1 - \eta_C} & \xi = 1 \\ 1 + (\eta_C^{-1} - 1) \ln(1 - \eta_C) & \xi \rightarrow \infty \\ 1 + \eta_C \ln^{-1}(1 - \eta_C) & \xi \rightarrow 0 \end{cases} \quad (11)$$

It is worth mentioning that, in the symmetry case, η_{EMW} is just the C-A efficiency[33], which is the EMP of a symmetry Carnot engine and has been obtained in many finite-time thermodynamics model [31, 38, 61, 62]. The maximum EMW in this case is achieved with infinite low-temperature source size of $\xi \rightarrow \infty$. The results of Eq. (11) have also been reported in [47] with constant heat capacity. And we find these η_{EMW} in different limits of ξ have the same coefficient in the first order of η_C , namely, $\eta_{\text{EMW}} = \eta_C/2 + O(\eta_C^2)$, which shares the same universality with EMP [31, 38]

B. low temperature regime

Different from the above case within the high-temperature regime, the capacity of the heat sources in the low-temperature regime of $T/\Theta \ll 1$, according to the Debye's law, follows $C_{H,L}(T) = \Lambda_{H,L}T^n$. The reversible condition of Eq. (8) in this case becomes

$$\int_0^{t_f} \Lambda_L T_L^{n-1} dT_L + \int_0^{t_f} \Lambda_H T_H^{n-1} dT_H = 0, \quad (12)$$

namely,

$$\Lambda_L (T_E^n - T_L^n) = \Lambda_H (T_H^n - T_E^n), \quad (13)$$

which gives the equilibrium temperature

$$T_E = \left(\frac{T_H^n + \xi T_L^n}{1 + \xi} \right)^{\frac{1}{n}} \quad (14)$$

with the capacity ratio reduces to $\xi = \Lambda_L/\Lambda_H$. Combining Eqs. (14) and (5), the EMW at low temperature regime reads

$$\eta_{\text{EMW}} = 1 - \frac{\xi\chi - \xi(1 - \eta_C)^{n+1}}{1 - \chi}, \quad (15)$$

where

$$\chi = \left[\frac{1 + \xi(1 - \eta_C)^n}{1 + \xi} \right]^{\frac{n+1}{n}} \quad (16)$$

In the limit of infinite low-temperature source size ($\xi \rightarrow \infty$), keeping the first order of ξ^{-1} in χ , we obtain

$$\eta_{\text{EMW}}(\xi \rightarrow \infty) = 1 - \frac{n+1}{n} \left[1 - \frac{\eta_C}{1 - (1 - \eta_C)^{n+1}} \right]. \quad (17)$$

On the other hand, in the case with infinite high-temperature source size ($\xi \rightarrow 0$), we expand χ up to the first order of ξ and find that

$$\eta_{\text{EMW}}(\xi \rightarrow 0) = 1 - \frac{n}{n+1} \left[\frac{1 - (1 - \eta_C)^{n+1}}{1 - (1 - \eta_C)^n} \right] \quad (18)$$

In Fig. 3, the EMW in these two limit cases are plotted as the function of η_C . The curves shows that $\eta_{\text{EMW}}(\xi \rightarrow \infty)$, the upper bound of η_{EMW} , increases with the heat source dimension n ; while the lower bound of η_{EMW} , i.e., $\eta_{\text{EMW}}(\xi \rightarrow 0)$ decreases with n . This means we can use high-dimension heat source with the low-temperature source much larger than the high-temperature one to realize higher efficiency.

Particularly, when the considered heat source is one-dimensional, i.e., $n = 1$, Eq. (15) is directly simplified as

$$\eta_{\text{EMW}}(n = 1) = \frac{\eta_C}{2 - \kappa\eta_C}, \quad (19)$$

where $\kappa = \xi/(1 + \xi)$, $\kappa \in (0, \infty)$. Since $\eta_{\text{EMW}}(n = 1)$ is a monotonically increasing function of κ , we conclude that

$$\eta_U \equiv \frac{\eta_C}{2} \leq \eta_{\text{EMW}}(n = 1) \leq \frac{\eta_C}{2 - \eta_C} \equiv \eta_L. \quad (20)$$

Interestingly, the upper and lower bound $\eta_{U,L}$ here are exactly the same as the bounds for the EMP obtained

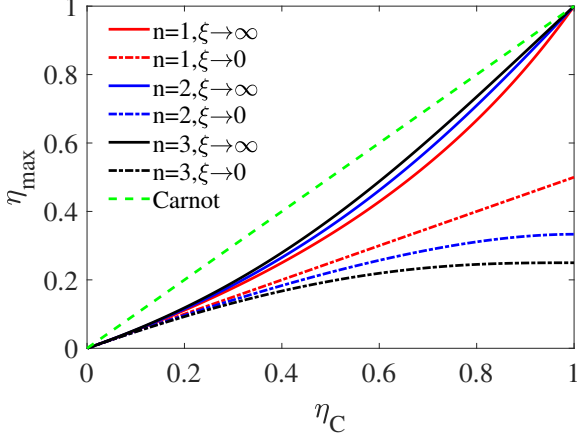


Figure 3. EMW η_{EMW} as the function of η_C with different source dimension n . The curve relates to infinite low-temperature source size ($\xi \rightarrow \infty$) and infinite high-temperature source size ($\xi \rightarrow 0$) are given by Eq. (17) and Eq. (18) respectively.

with different finite-time heat engine models [31, 38, 61]. Similar result has been found by [52] with the energy-entropy relation. In addition, in the limit of $\eta_C \rightarrow 1$, the lower bound of η_{EMW} in Eq. (18) is found to be only determined by the heat source dimension, i.e.,

$$\lim_{\eta_C \rightarrow 1} \eta_{\text{EMW}} (\xi \rightarrow 0) = \frac{1}{n+1}. \quad (21)$$

This phenomenon is observed in Fig. 3, where the intersection of the three dash-dotted lines and $\eta_C = 1$ are, from top to bottom, $\eta_{\text{EMW}} = 1/2$, $\eta_{\text{EMW}} = 1/3$, and $\eta_{\text{EMW}} = 1/4$ respectively. Moreover, up to the first order of η_C , an universality is found the general result of EMW both in the high and low temperature regime, namely,

$$\eta_{\text{EMW}} = \frac{\eta_C}{2} + O(\eta_C^2). \quad (22)$$

The same universality has been discovered before for EMP [31, 38].

For those systems that do not satisfy the Debye's law, we can first derive the heat capacity as the function of temperature from its energy spectrum and the corresponding equilibrium population. Then taking using of Eqs. (14) and (8) to obtain the EMW in quasi-static limit. It should be mentioned that the general result of Eq. (15) is also suitable for Fermi gas at low temperature and photon gas (black body radiation) by taking $n = 1$ and $n = 3$ respectively. Since the capacity of the former follows $C_{\text{FG}}(T) \propto T$, while $C_{\text{PG}}(T) \propto T^3$ for the latter [63].

III. FINITE-TIME PERFORMANCE OF THE HEAT ENGINE

In the previous section, we derive the EMW that heat engines can achieve under the reversible condition, which is satisfied by a quasi-static cycle with vanishing output power. In this section, we extend our discussion in Sec. II to the finite-time case [49, 50]. Unlike the optimization goal of Ref [49, 50], where the efficiency at maximum time-average power of the whole process is studied, we focus on how efficient the engine can be when the power of each cycle is maximized. We assume the engine can run N cycle from $t = 0$ to the stop time $t = t_f$, where $N \gg 1$ but finite as we mentioned before. The operation time of the i -th cycle ($i = 1, 2, \dots, N$) begins at $t = t_i$ is denoted as $\tau_i = t_{i+1} - t_i$. The efficiency of the whole process then reads

$$\eta = 1 - \frac{\sum_{i=1}^N \Delta Q_C^{(i)}}{\sum_{i=1}^N \Delta Q_H^{(i)}}, \quad (23)$$

where $\Delta Q_H^{(i)} = -\int_{t_i}^{t_{i+1}} dQ_H$ and $\Delta Q_C^{(i)} = \int_{t_i}^{t_{i+1}} dQ_C$. In the i -th cycle, the output power is $P^{(i)} = (\Delta Q_H^{(i)} - \Delta Q_C^{(i)}) \tau_i^{-1}$. Below we try to obtain the upper and lower bounds for η under the condition that the maximum $P^{(i)}$ is achieved in each cycle. Suppose the heat engine works in the Carnot-like cycle, which contains two adiabatic processes and two finite-time isothermal process. In the finite-time isothermal processes, the heat transfer generally follows, in the i -th cycle,

$$\Delta Q_H^{(i)} = T_H^{(i)} (\Delta S_{\text{re}}^{(i)} - \Delta S_{\text{irr,H}}^{(i)}), \quad (24)$$

$$\Delta Q_C^{(i)} = T_C^{(i)} (\Delta S_{\text{re}}^{(i)} + \Delta S_{\text{irr,C}}^{(i)}). \quad (25)$$

Here, $T_H^{(i)}$ ($T_C^{(i)}$) is the temperature of the high (low) temperature heat source, $\Delta S_{\text{re}}^{(i)}$ is reversible entropy change, and $\Delta S_{\text{irr},\alpha}^{(i)}$ ($\alpha = \text{H, C}$) is the irreversible entropy generation relates to the corresponding source. With the low-dissipation assumption, as suggested first by [38], the irreversible entropy follows the $1/\tau$ relation as $\Delta S_{\text{irr},\alpha}^{(i)} = \Sigma_\alpha^{(i)} / \tau_\alpha^{(i)}$, where $\Sigma_\alpha^{(i)}$ depends on the dissipative feature of the working substance when contacting with the heat source [43] and $\tau_\alpha^{(i)}$ is the operation time of the corresponding process. Such relation has been proved for both classical [64] and quantum system [43, 44] and was recently observed in the experiment [45]. Applying straightforward optimization of $P^{(i)}(\tau_H^{(i)}, \tau_C^{(i)})$ with respect to $\tau_H^{(i)}$ and $\tau_C^{(i)}$, the EMP in the i -th cycle is obtained as [38] (See App. A for detailed derivation)

$$\eta_{\text{EMP}}^{(i)} = \frac{\eta_C^{(i)}}{2 - \gamma^{(i)} \eta_C^{(i)}} \quad (26)$$

with

$$\gamma^{(i)} = \left(1 + \sqrt{\frac{T_C^{(i)} \Sigma_C^{(i)}}{T_H^{(i)} \Sigma_H^{(i)}}} \right)^{-1} \quad (27)$$

and $\eta_C^{(i)} = 1 - T_C^{(i)}/T_H^{(i)}$ being the Carnot efficiency determined by the temperature of the sources in the i -th cycle. When the maximum power output for each cycle is achieved, the efficiency of Eq. (23), denoted as η^{FT} , becomes

$$\eta^{\text{FT}} = \frac{\sum_{i=1}^N \eta_{\text{EMP}}^{(i)} \Delta Q_H^{(i)}}{\sum_{i=1}^N \Delta Q_H^{(i)}}, \quad (28)$$

which is a monotonically increasing function of $\eta_{\text{EMP}}^{(i)}$. Note that $\eta_{\text{EMP}}^{(i)}$ is bounded by $\eta_{\pm}^{(i)}$ as

$$\eta_-^{(i)} \equiv \frac{\eta_C^{(i)}}{2} \leq \eta_{\text{EMP}}^{(i)} \leq \frac{\eta_C^{(i)}}{2 - \eta_C^{(i)}} \equiv \eta_+^{(i)}, \quad (29)$$

where the upper bound and lower bound are achieved respectively by taking the limit of $\gamma \rightarrow 1$ ($\Sigma_C^{(i)} \rightarrow 0$) and $\gamma \rightarrow 0$ ($\Sigma_H^{(i)} \rightarrow 0$). Therefore,

$$\frac{\sum_{i=1}^N \eta_-^{(i)} \Delta Q_H^{(i)}}{\sum_{i=1}^N \Delta Q_H^{(i)}} \leq \eta^{\text{FT}} \leq \frac{\sum_{i=1}^N \eta_+^{(i)} \Delta Q_H^{(i)}}{\sum_{i=1}^N \Delta Q_H^{(i)}}. \quad (30)$$

In the following, we will derive upper and lower bound for efficiency of Eq. (30). In the limit of $\gamma \rightarrow 1$, the upper bound of Eq. (30)

$$\frac{\sum_{i=1}^N \eta_+^{(i)} \Delta Q_H^{(i)}}{\sum_{i=1}^N \Delta Q_H^{(i)}} \equiv \eta_U^{\text{FT}}. \quad (31)$$

For simplicity, we only consider the heat source with constant heat capacity in the following. As we studied in Sec. II, the EMW in the reversible situation is bounded as $\eta_{\text{EMW}}(\xi \rightarrow 0) \leq \eta_{\text{EMW}} \leq \eta_{\text{EMW}}(\xi \rightarrow \infty)$ (See Eq. (11)). Therefore, to achieve higher efficiency in finite time, we should focus on the case of $\xi \rightarrow \infty$, where the low-temperature source is much larger than the high-temperature one. Such that the cold source is kept at a constant temperature in the whole the process, i.e., $T_C^{(i)} = T_C$ and the hot source temperature rises with time until $T_H^{(N)} = T_C$ and the heat engine stops working. Substituting Eq. (B2) into Eq. (31), and replace the sum by integral with $N \gg 1$, we obtain

$$\eta_U^{\text{FT}} = \frac{\int_0^{t_f} \frac{\eta_C(t)}{2 - \eta_C(t)} dQ_H}{\int_0^{t_f} dQ_H}, \quad (32)$$

which can be further simplified as, noticing $\eta_C(t) = 1 - T_C/T_H(t)$ and $dQ_H = C_H dT_H$,

$$\eta_U^{\text{FT}} = \frac{\int_{T_H}^{T_C} \frac{T_H(t) - T_C}{T_H(t) + T_C} dT_H}{\int_{T_H}^{T_C} dT_H}, \quad (33)$$

After finishing the integral, the upper bound for efficiency is finally found as, in terms of the initial Carnot efficiency η_C ,

$$\eta_U^{\text{FT}}(\xi \rightarrow \infty) = 1 - \frac{2(1 - \eta_C)}{\eta_C} \ln \frac{2 - \eta_C}{2(1 - \eta_C)}. \quad (34)$$

Similarly, for $\gamma \rightarrow 0$, by replacing $\eta_+(t)$ in Eq. (32) with $\eta_-(t) = \eta_C(t)/2$, we find

$$\eta_L^{\text{FT}}(\xi \rightarrow \infty) = \frac{1}{2} [1 + (\eta_C^{-1} - 1) \ln(1 - \eta_C)], \quad (35)$$

which is exactly half of $\eta_{\text{EMW}}(\xi \rightarrow \infty)$ in the reversible case. And the detailed derivations of other two bounds in the limit of $\xi \rightarrow 0$ are given in App. B. Here we make a brief summary of the efficiency bounds obtained in different limit as follows

$$\eta_U^{\text{FT}}(\xi \rightarrow \infty) = 1 + \frac{2(1 - \eta_C)}{\eta_C} \ln \frac{2(1 - \eta_C)}{2 - \eta_C}, \quad (36)$$

$$\eta_L^{\text{FT}}(\xi \rightarrow \infty) = \frac{\eta_{\text{EMW}}(\xi \rightarrow \infty)}{2}, \quad (37)$$

$$\eta_U^{\text{FT}}(\xi \rightarrow 0) = \frac{\eta_{\text{EMW}}(\xi \rightarrow 0)}{2 - \eta_{\text{EMW}}(\xi \rightarrow 0)}, \quad (38)$$

$$\eta_L^{\text{FT}}(\xi \rightarrow 0) = 1 + \frac{\eta_C}{2} \ln^{-1} \left(1 - \frac{\eta_C}{2} \right), \quad (39)$$

where $\eta_{\text{EMP}}(\xi \rightarrow \infty)$ and $\eta_{\text{EMP}}(\xi \rightarrow 0)$ are the corresponding efficiency in the reversible limit as given by Eq. (11). Interestingly, the dependence of η on η_{EMW} in the limit of $(\xi \rightarrow \infty, \gamma \rightarrow 0)$ and $(\xi \rightarrow 0, \gamma \rightarrow 1)$ follows the same form as its corresponding counterpart in the infinite heat source case. These efficiency in different limit of ξ and γ are illustrated in Fig. 4 with the solid lines, where the dashed lines are the upper and lower bounds of EMP, i.e., $\eta_{\text{EMP}}(\xi \rightarrow \infty)$ and $\eta_{\text{EMP}}(\xi \rightarrow 0)$. It's easily to check that these efficiency follow the universality as

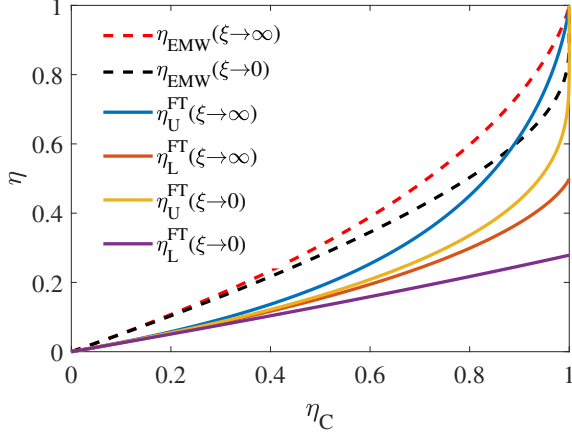


Figure 4. Upper (η_U^{FT}) and lower (η_L^{FT}) bounds for efficiency of the heat engine in finite-time operation as the function of η_C in different limit of ξ . η_U^{FT} and η_L^{FT} respectively corresponds to $\gamma \rightarrow 1$ and $\gamma \rightarrow 0$. Here ξ and γ respectively characterize the asymmetry in size and dissipation of the two heat sources. As the comparison, the red(black) dashed line represent the upper (lower) bound of EMP in the reversible limit given by Eq. (11). Other are plotted with Eqs. (36), (37), (38), and (39).

$$\eta = \frac{\eta_C}{4} + O(\eta_C^2). \quad (40)$$

Comparing the above universality with Eq. (22), we can also write the universality of η in term of η_{EMW} as

$$\eta = \frac{\eta_{\text{EMW}}}{2} + O(\eta_{\text{EMW}}^2), \quad (41)$$

which means that, up to the first order of η_C , the efficiency when the power of each cycle is maximized is just half of the EMW. Such universality is also found for the efficiency at maximum time-average power with linear irreversible heat engine under the tight coupling condition [49, 50].

IV. BLACK HOLES SERVED AS HEAT SOURCES

In the previous section, We have discussed the situation that heat engine operates to stop between two finite-size heat sources when the high-temperature and low-temperature source reach the same temperature. This actually based on the assumption that the heat capacity of the heat sources are positive as we mentioned before, such that the temperature of the high-temperature heat source is lowered and the temperature of the low-temperature heat source is increased as the engine's working. Although most physical systems have positive heat capacity, there are indeed some systems with negative heat capacity, i.e., $C = \partial U / \partial T < 0$, such as black holes [65, 66].

All the thermodynamic properties of a black hole only rely on its mass M , angular momentum J , and charge Q , known as the three hairs of black hole [66]. For simplicity, we consider the Schwarzschild black hole, which only has one hair, the mass. The internal energy and temperature of a Schwarzschild black hole B with mass M are respectively $U = M$ and $T = 1/(8\pi M)$. Here and after, we use the natural unit system. Therefore, the heat capacity of B is $C = \partial U / \partial T = -8\pi M^2$. Obviously, such heat capacity is negative and increases quadratically with the black hole's mass.

Now we consider two Schwarzschild black holes of mass M_H and M_L served as high and low temperature heat source respectively. Note the high temperature black hole has smaller mass, than the low temperature one, namely, $M_H < M_L$. The working substance reciprocates between the two black holes and exchanges heat as well as output work, and we ignore the influence of gravity on the cycle process in the following discussion. After the heat engine absorbs heat from the high temperature black hole, the mass of the high temperature black hole decreases, i.e., $M_H \downarrow$ and then its temperature rises, namely $T_H \uparrow$; and when the heat is released to the low-temperature black hole, the mass $M_C \uparrow$ and the temperature $T_H \downarrow$ consequently. This is exactly the opposite of what we discussed for the positive heat capacity bath. Thus, the condition that the heat engine stops working is no longer the temperature convergence of the two heat sources ($T_L(t_f) = T_H(t_f) \equiv T_E$), but the high temperature heat source, i.e., the smaller black hole, is exhausted, namely, $M_H(t_f) = 0$. As a result, the efficiency of the heat engine work between these two black holes follows

$$\eta = 1 - \frac{M_L(t_f) - M_L}{M_H}. \quad (42)$$

Here we have assumed that the black holes only exchange heat with the working substance without external energy transfer channels. We still consider the reversible cycle for convenient, and the reversible condition of Eq. (8) now becomes

$$\int_0^{t_f} \frac{dM_H}{1/(8\pi M_H)} + \int_0^{t_f} \frac{dM_L}{1/(8\pi M_L)} = 0 \quad (43)$$

Then we obtain

$$M_H^2 + M_L^2 = M_L^2(t_f). \quad (44)$$

The above formula can also be derived with the conservation of black hole area entropy with no information loss [67–70] as

$$\sum_{\alpha=H,C} S_{\text{BH}}(M_\alpha) = \sum_{\alpha=H,C} S_{\text{BH}}[M_\alpha(t_f)] \quad (45)$$

with $S_{\text{BH}}(M) = 4\pi M^2$ being the Beckenstein-Hawking Entropy. Combining Eqs. (42) and (44), the EMW reads

$$\eta_{\text{EMW}} = \frac{\eta_C + \sqrt{(1 - \eta_C)^2 + 1}}{1 + \sqrt{(1 - \eta_C)^2 + 1}} \geq \eta_C, \quad (46)$$

where

$$\eta_C = 1 - \frac{T_L}{T_H} = 1 - \frac{M_H}{M_C} \quad (47)$$

is the Carnot efficiency defined by the initial mass of the two black holes. As demonstrated by Eq. (42), the maximum η_{max} can surpass the initial Carnot efficiency due to the unusual nature of negative heat capacity of black hole. η_{EMW} as the function of η_C is plotted in Fig. 5. We should emphasize here that this result does not violate the second law of thermodynamics, because the temperature of the two black holes are not constant, but has an increasing temperature difference as the heat engine works. Moreover, compared with the result relates to positive heat capacity sources in Eqs. (10) and (15), the EMP of Eq. (46) only rely on the initial Carnot efficiency without relying on other parameters. We can regard this phenomenon as the embodiment of the No-hair theorem [66] in efficiency for heat engines operating between black holes.

When the initial mass of the two black holes are the same, i.e., $T_L = T_H$ and $\eta_C = 0$, the heat engine can be driven with some energy fluctuation between the working substance and one of the black hole due to the Hawking radiation process [71, 72], in such circumstance, one has

$$\lim_{\eta_C \rightarrow 0} \eta_{\text{EMW}} = 2 - \sqrt{2}. \quad (48)$$

This is two times of the maximum energy release rate $\mu = (2 - \sqrt{2})/2 \approx 0.29$ of two black holes' emerging process which was first derived by Hawking[73]. We note that there are studies that have linked black holes to heat engines[74–76]. However, to our best knowledge, these works mainly consider the black holes as the working substance rather than heat sources, and do not consider the finite-size effect.

Besides the black hole, the negative heat capacity also been observed in some Cluster of atom system with phase transition [77–79]. The discussion in this section can be extends to these systems, we hope to use these novel materials to achieve high energy conversion efficiency in the near future.

V. CONCLUSION AND DISCUSSION

In summary, we studied the efficiency of a heat engine working between two finite-size heat source in both

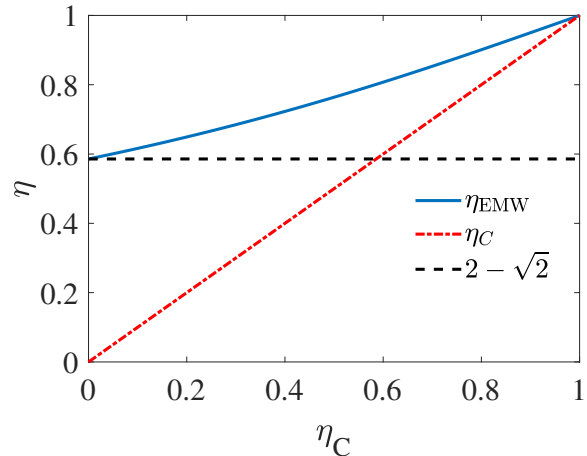


Figure 5. EMW of a heat engine working between two Schwarzschild black holes

quasi-static and finite-time cases. The effect of the heat capacity of the finite-size heat source on the engine's efficiency is clarified. When the engine operates in quasi-static cycles, with the assumption that the source's capacity follows the Debye's law, we obtained the corresponding efficiency at maximum work (EMW) in the high and low temperature regime, as given by Eq. (10) and Eq. (15) respectively. In addition, we also find some bounds for such EMW in different circumstances [Eq. (11) of high temperature regime and Eqs. (17) and (18) for low temperature]. We proved that, in the low temperature case, with the limit of $\eta_C \rightarrow 1$, the lower bound of η_{EMW} only determined by the heat source's dimension, i.e., $\lim_{\eta_C \rightarrow 1} \eta_{\text{EMW}}(\xi \rightarrow 0) = (n + 1)^{-1}$. And for the 1-dimensional sources, the upper and lower bound $\eta_U = \eta_C(2 - \eta_C)^{-1}$ and $\eta_L = \eta_C/2$ of η_{EMW} are exactly the same as the bounds for the efficiency at maximum power (EMP) obtained with several finite-time heat engine models [31, 38, 61].

For the heat engine working within finite time, we modeled the engine as a low-dissipation Carnot-like engine and studied the efficiency with the output power of each cycle is maximized. A series of bounds for the efficiency are obtained in Eqs. (36), (37), (38), and (39) and plotted in Fig. 4, where the overall upper bound is achieved with $\xi \rightarrow \infty, \gamma \rightarrow 1$, namely, the size of cold source is much larger than that of the hot one while the dissipation of the cold source approaches vanishing. An universality is found for all these bounds obtained with finite-size sources and finite-time as $\eta = \eta_C/4 + O(\eta_C^2)$, where the coefficient of η_C 's first order is just half of that of the EMP.

Although we have discussed the effect of asymmetry in the size of the hot and cold sources on the efficiency, the results are obtained for the heat capacity function rely on temperature of the sources share the same form. Considering that the high and low temperature heat

sources have different temperature dependence, such as cold source's heat capacity varies with temperature following the power law while the capacity of the hot source heat capacity remains constant, etc., is a potential direction for the optimization of the heat engine's performance. In addition, the effect of phase transition (PT) is also worth exploring in future study, as the heat capacity of sources with PT may have completely different characteristics in different phases due to temperature changes.

In the last part of this paper, we studied an unusual case where the sources have negative heat capacity. Using black hole as a demonstration, we obtain the EMW for a heat engine working between two Schwarzschild black holes as shown in Eq. (5). The EMP is found always higher than the initial Carnot efficiency defined by the initial mass of the two black holes. But we emphasize that this does not violate the second law of thermodynamics, since the temperature of the two black hole are not constant but has an increasing temperature difference as the heat engine operates due to the negative heat capacity of the sources. In addition, even when the initial mass of the two black holes are the same, the heat engine can be driven with some energy fluctuation between the working substance and one of the black hole from the Hawking radiation process. In this situation, the EMW is proved to be $\eta_{\text{EMW}} = 2 - \sqrt{2} = 2\mu$, where

$\mu = (2 - \sqrt{2})/2 \approx 0.29$ is the maximum energy release rate of two black holes' emerging process discovered by S. Hawking [73]. The discussions about this issue in this paper are limited to quasi-static heat engines working between the Schwarzschild black holes, and the black holes only exchange heat with the working substance without external energy transfer. Considering the finite-time effect, the non-negligible energy loss due to the Hawking radiation, the cases with other types of black holes, and the gravitational effect on the efficiency of the heat engine will be a series of interesting and challenging tasks, which will be investigated in our further studies. Moreover, since there have been some experimental reports on negative heat capacity materials [77–79], it is feasible to take use of these materials as heat sources providing energy for the heat engines to test our predictions.

ACKNOWLEDGMENTS

This work is supported by the NSFC (Grants No. 11534002 and No. 11875049), the NSAF (Grant No. U1730449 and No. U1530401), and the National Basic Research Program of China (Grants No. 2016YFA0301201 and No. 2014CB921403). The author thanks Yun-He Zhao of Capital Normal University High School for carefully proofreading of this paper.

-
- [1] K. Huang, *Introduction To Statistical Physics, 2Nd Edition* (T&F/Crc Press, 2013), ISBN 978-1-4200-7902-9.
 - [2] M. Esposito, U. Harbola, and S. Mukamel, *Rev. Mod. Phys.* **81**, 1665 (2009).
 - [3] M. Campisi, P. Hänggi, and P. Talkner, *Rev. Mod. Phys.* **83**, 771 (2011).
 - [4] R. Kosloff and A. Levy, *Annual Review of Physical Chemistry* **65**, 365 (2014).
 - [5] J. P. Pekola, *Nat. Phys.* **11**, 118 (2015).
 - [6] S. Vinjanampathy and J. Anders, *Contemp. Phys.* **57**, 545 (2016).
 - [7] F. Binder, L. A. Correa, C. Gogolin, J. Anders, and G. Adesso, eds., *Thermodynamics in the Quantum Regime* (Springer International Publishing, 2018).
 - [8] R. Kosloff, *The Journal of chemical physics* **150**, 204105 (2019).
 - [9] H. Scovil and E. Schulz-DuBois, *Physical Review Letters* **2**, 262 (1959).
 - [10] R. Alicki, *Journal of Physics A: Mathematical and General* **12**, L103 (1979).
 - [11] R. Kosloff, *The Journal of chemical physics* **80**, 1625 (1984).
 - [12] M. O. Scully, M. S. Zubairy, G. S. Agarwal, and H. Walther, *Science* **299**, 862 (2003).
 - [13] H. T. Quan, Y. xi Liu, C. P. Sun, and F. Nori, *Phys. Rev. E* **76** (2007).
 - [14] J.-P. Brantut, C. Grenier, J. Meineke, D. Stadler, S. Krinner, C. Kollath, T. Esslinger, and A. Georges, *Science* **342**, 713 (2013).
 - [15] A. Dechant, N. Kiesel, and E. Lutz, *Physical Review Letters* **114** (2015).
 - [16] J. Rossnagel, S. T. Dawkins, K. N. Tolazzi, O. Abah, E. Lutz, F. Schmidt-Kaler, and K. Singer, *Science* **352**, 325 (2016).
 - [17] O. Abah and E. Lutz, *Physical Review E* **98** (2018).
 - [18] M. Passos, A. C. Santos, M. S. Sarandy, and J. Huguenin, *Physical Review A* **100**, 022113 (2019).
 - [19] O. Fialko and D. W. Hallwood, *Phys. Rev. Lett.* **108** (2012).
 - [20] J. Rossnagel, O. Abah, F. Schmidt-Kaler, K. Singer, and E. Lutz, *Physical Review Letters* **112** (2014).
 - [21] Y.-H. Ma, S.-H. Su, and C.-P. Sun, *Phys. Rev. E* **96** (2017).
 - [22] K. Brandner, M. Bauer, and U. Seifert, *Physical Review Letters* **119** (2017).
 - [23] S. Su, J. Chen, Y. Ma, J. Chen, and C. Sun, *Chinese Physics B* **27**, 060502 (2018).
 - [24] K. E. Dorfman, D. Xu, and J. Cao, *Physical Review E* **97**, 042120 (2018).
 - [25] P. A. Camati, J. F. G. Santos, and R. M. Serra, *Physical Review A* **99** (2019).
 - [26] J.-F. Chen, C.-P. Sun, and H. Dong, *Physical Review E* **100**, 032144 (2019).
 - [27] S. R. De Groot and P. Mazur, *Non-equilibrium thermodynamics* (Courier Corporation, 2013).
 - [28] B. Andresen, *Finite-time thermodynamics* (University of Copenhagen Copenhagen, 1983).
 - [29] B. Andresen, R. S. Berry, M. J. Ondrechen, and P. Salamon, *Accounts of Chemical Research* **17**, 266 (1984).
 - [30] C. Wu, *Recent advances in finite-time thermodynamics*

- (Nova Publishers, 1999).
- [31] Z.-C. Tu, Chinese Physics B **21**, 020513 (2012).
 - [32] V. Holubec and A. Ryabov, Physical Review E **96** (2017).
 - [33] F. L. Curzon and B. Ahlborn, Am. J. Phys. **43**, 22 (1975).
 - [34] B. Andresen, R. S. Berry, A. Nitzan, and P. Salamon, Physical Review A **15**, 2086 (1977).
 - [35] J. Chen, Journal of Physics D: Applied Physics **27**, 1144 (1994).
 - [36] K. Sekimoto and S. ichi Sasa, Journal of the Physical Society of Japan **66**, 3326 (1997).
 - [37] C. V. den Broeck, Physical Review Letters **95** (2005).
 - [38] M. Esposito, R. Kawai, K. Lindenberg, and C. V. den Broeck, Physical Review Letters **105** (2010).
 - [39] Z. C. Tu, J. Phys. A: Math. Theor. **41**, 312003 (2008).
 - [40] V. Holubec and A. Ryabov, Journal of Statistical Mechanics: Theory and Experiment **2016**, 073204 (2016).
 - [41] N. Shiraishi, K. Saito, and H. Tasaki, Physical Review Letters **117** (2016).
 - [42] V. Cavina, A. Mari, and V. Giovannetti, Physical Review Letters **119** (2017).
 - [43] Y.-H. Ma, D. Xu, H. Dong, and C.-P. Sun, Physical Review E **98** (2018).
 - [44] Y.-H. Ma, D. Xu, H. Dong, and C.-P. Sun, Physical Review E **98** (2018).
 - [45] Y.-H. Ma, R.-X. Zhai, C.-P. Sun, and H. Dong, arXiv preprint arXiv:1910.13434 (2019).
 - [46] M. J. Ondrechen, B. Andresen, M. Mozurkewich, and R. S. Berry, American Journal of Physics **49**, 681 (1981).
 - [47] M. J. Ondrechen, M. H. Rubin, and Y. B. Band, The Journal of Chemical Physics **78**, 4721 (1983).
 - [48] H. S. Leff, American Journal of Physics **55**, 701 (1987).
 - [49] Y. Izumida and K. Okuda, Physical review letters **112**, 180603 (2014).
 - [50] Y. Wang, Physical Review E **90**, 062140 (2014).
 - [51] R. S. Johal, Physical Review E **94**, 012123 (2016).
 - [52] R. S. Johal and R. Rai, EPL (Europhysics Letters) **113**, 10006 (2016).
 - [53] H. Tajima and M. Hayashi, Physical Review E **96**, 012128 (2017).
 - [54] C. Sparaciari, J. Oppenheim, and T. Fritz, Physical Review A **96**, 052112 (2017).
 - [55] J. G. Richens, Á. M. Alhambra, and L. Masanes, Physical Review E **97**, 062132 (2018).
 - [56] A. Pozas-Kerstjens, E. G. Brown, and K. V. Hovhannisyan, New Journal of Physics **20**, 043034 (2018).
 - [57] M. H. Mohammady and A. Romito, arXiv preprint arXiv:1902.09378 (2019).
 - [58] F. Barra, Physical Review Letters **122**, 210601 (2019).
 - [59] H. S. Leff, American Journal of Physics **55**, 602 (1987).
 - [60] C. Kittel et al., *Introduction to solid state physics*, vol. 8 (Wiley New York, 1976).
 - [61] T. Schmiedl and U. Seifert, EPL (Europhysics Letters) **83**, 30005 (2008).
 - [62] R. S. Johal and A. M. Jayannavar, arXiv preprint arXiv:1903.04381 (2019).
 - [63] R. Pathria and P. BEALE, *Statistical mechanics. [sl]* (1996).
 - [64] P. Salamon, A. Nitzan, B. Andresen, and R. S. Berry, Physical Review A **21**, 2115 (1980).
 - [65] E. F. Taylor and J. A. Wheeler (1975).
 - [66] J. D. Bekenstein, Physics Today **33**, 24 (1980).
 - [67] M. K. Parikh and F. Wilczek, Physical Review Letters **85**, 5042 (2000).
 - [68] B. Zhang, Q.-y. Cai, L. You, and M.-s. Zhan, Physics Letters B **675**, 98 (2009).
 - [69] Y.-H. Ma, Q.-Y. Cai, H. Dong, and C.-P. Sun, EPL (Europhysics Letters) **122**, 30001 (2018).
 - [70] Y.-H. Ma, J.-F. Chen, and C.-P. Sun, Nuclear Physics B **931**, 418 (2018).
 - [71] S. W. Hawking, Nature **248**, 30 (1974).
 - [72] S. W. Hawking, Communications in mathematical physics **43**, 199 (1975).
 - [73] S. W. Hawking, Physical Review Letters **26**, 1344 (1971).
 - [74] C. V. Johnson, Classical and Quantum Gravity **31**, 205002 (2014).
 - [75] S. Hendi, B. E. Panah, S. Panahiyan, H. Liu, and X.-H. Meng, Physics Letters B **781**, 40 (2018).
 - [76] S.-W. Wei and Y.-X. Liu, Nuclear Physics B **946**, 114700 (2019).
 - [77] M. d'Agostino, F. Gulminelli, P. Chomaz, M. Bruno, F. Cannata, R. Bougault, F. Gramegna, I. Iori, N. Le Neindre, G. Margagliotti, et al., Physics Letters B **473**, 219 (2000).
 - [78] M. Schmidt, R. Kusche, T. Hippler, J. Donges, W. Krommüller, B. Von Issendorff, and H. Haberland, Physical review letters **86**, 1191 (2001).
 - [79] J. A. Reyes-Nava, I. L. Garzón, and K. Michaelian, Physical Review B **67**, 165401 (2003).

Appendix A: Optimization of low-dissipation Carnot-like engine

In this Appendix, we briefly show the optimization of the low-dissipation Carnot-like engine introduced in Sec. III, we follow the same optimization method in Ref. [38]. For such engine working in the i -th Carnot-like cycle, the heat transfer in the two finite-time isothermal processes read

$$\Delta Q_H^{(i)} = T_H^{(i)} \left(\Delta S_{\text{re}}^{(i)} - \frac{\Sigma_H^{(i)}}{\tau_H^{(i)}} \right), \quad (\text{A1})$$

and

$$\Delta Q_C^{(i)} = T_C^{(i)} \left(\Delta S_{\text{re}}^{(i)} + \frac{\Sigma_C^{(i)}}{\tau_C^{(i)}} \right), \quad (\text{A2})$$

where, $T_H^{(i)} (T_C^{(i)})$ is the temperature of the high (low) temperature heat source, $\Delta S_{\text{re}}^{(i)}$ is reversible entropy change, $\Sigma_\alpha^{(i)}$ depends on the dissipative nature of the working substance when contacting with the heat source and $\tau_\alpha^{(i)}$ is the corresponding operation time. Thus, the efficiency and power of the engine for the i -th cycle follows

$$\eta^{(i)} = \frac{\Delta Q_H^{(i)} - \Delta Q_C^{(i)}}{\Delta Q_H^{(i)}} \quad (\text{A3})$$

$$= \frac{\left(T_H^{(i)} - T_C^{(i)}\right) \Delta S_{\text{re}}^{(i)} - \frac{\Sigma_H^{(i)}}{\tau_H^{(i)}} - \frac{\Sigma_C^{(i)}}{\tau_C^{(i)}}}{T_H^{(i)} \left(\Delta S_{\text{re}}^{(i)} - \frac{\Sigma_H^{(i)}}{\tau_H^{(i)}}\right)} \quad (\text{A4})$$

and

$$P^{(i)} = \frac{\Delta Q_H^{(i)} - \Delta Q_C^{(i)}}{\tau_H^{(i)} + \tau_C^{(i)}} \quad (\text{A5})$$

$$= \frac{\left(T_H^{(i)} - T_C^{(i)}\right) \Delta S_{\text{re}}^{(i)} - \frac{\Sigma_H^{(i)}}{\tau_H^{(i)}} - \frac{\Sigma_C^{(i)}}{\tau_C^{(i)}}}{\tau_H^{(i)} + \tau_C^{(i)}} \quad (\text{A6})$$

Here the operation time in the two adiabatic processes are ignored [38]. The maximum power of each cycle is obtained by setting the derivatives of $P^{(i)} = P^{(i)}(\tau_H^{(i)}, \tau_C^{(i)})$ with respect to $\tau_H^{(i)}$ and $\tau_C^{(i)}$ equal to zero. Thus we find the corresponding times for the engine working at maximum power as

$$\tau_H^{(i)} = 2 \frac{T_H^{(i)} \Sigma_H^{(i)}}{\left(T_H^{(i)} - T_C^{(i)}\right) \Delta S_{\text{re}}^{(i)}} \left(1 + \sqrt{\frac{T_C^{(i)} \Sigma_C^{(i)}}{T_H^{(i)} \Sigma_H^{(i)}}}\right) \quad (\text{A7})$$

and

$$\tau_C^{(i)} = \tau_H^{(i)} \sqrt{\frac{T_C^{(i)} \Sigma_C^{(i)}}{T_H^{(i)} \Sigma_H^{(i)}}} \quad (\text{A8})$$

Substituting Eqs. (A7) and (A8) into Eq. (A4), the efficiency at maximum power is obtained as

$$\eta_{\text{EMP}}^{(i)} = \frac{\eta_C^{(i)}}{2 - \gamma^{(i)} \eta_C^{(i)}}, \quad (\text{A9})$$

where

$$\gamma^{(i)} = \left(1 + \sqrt{\frac{T_C^{(i)} \Sigma_C^{(i)}}{T_H^{(i)} \Sigma_H^{(i)}}}\right)^{-1} \quad (\text{A10})$$

and $\eta_C^{(i)} = 1 - T_C^{(i)}/T_H^{(i)}$ is the Carnot efficiency determined by the temperature of the sources in the i -th cycle

Appendix B: Bounds for efficiency in finite time in the limit of $\xi \rightarrow 0$

In this Appendix, we derive the upper and lower bounds for efficiency of heat engine working between

finite-size source within finite time in the limit of $\xi \rightarrow 0$. In this case, the cold source is much smaller than the hot one, thus $T_H^{(i)} = T_H$ and $T_C^{(N)} = T_H$ at $t = t_f$. In the limit of $\gamma \rightarrow 1$, the efficiency of Eq. (28) becomes

$$\eta = \frac{\sum_{i=1}^N \frac{\eta_C^{(i)}}{2 - \eta_C^{(i)}} \Delta Q_H^{(i)}}{\sum_{i=1}^N \Delta Q_H^{(i)}}. \quad (\text{B1})$$

Note that in this limit, Eqs. (A7) and (A8) respectively reduce to $\tau_H^{(i)} = 2\Sigma_H^{(i)}/(\eta_C^{(i)} \Delta S_{\text{re}}^{(i)})$ and $\tau_C^{(i)} = 0$, substituting which into Eq. (A1) and Eq. (A2), we find the relation between heat transfer and reversible entropy change as

$$\Delta Q_H^{(i)} = T_H^{(i)} \Delta S_{\text{re}}^{(i)} \left(1 - \frac{\eta_C^{(i)}}{2}\right). \quad (\text{B2})$$

and

$$\Delta Q_C^{(i)} = T_C^{(i)} \Delta S_{\text{re}}^{(i)}. \quad (\text{B3})$$

Using Eqs. (B2) and (B3), and replace the sum by integral with $N \gg 1$, Eq. (B1) is simplified as

$$\eta = \frac{\int_0^{t_f} \frac{\eta_C(t)}{2 - \eta_C(t)} \left[1 - \frac{\eta_C(t)}{2}\right] T_H dS_{\text{re}}}{\int_0^{t_f} \left[1 - \frac{\eta_C(t)}{2}\right] T_H dS_{\text{re}}} \quad (\text{B4})$$

$$= \frac{\int_0^{t_f} \eta_C(t) dS_{\text{re}}}{\int_0^{t_f} [2 - \eta_C(t)] dS_{\text{re}}} \quad (\text{B5})$$

$$= \frac{\int_{T_L}^{T_H} \eta_C(t) \left(\frac{C_L dT_L}{T_L}\right)}{\int_{T_L}^{T_H} [2 - \eta_C(t)] \left(\frac{C_L dT_L}{T_L}\right)} \quad (\text{B6})$$

$$= \frac{\int_{T_L}^{T_H} \left(\frac{T_H}{T_L} - 1\right) dT_L}{\int_{T_L}^{T_H} \left(\frac{T_H}{T_L} + 1\right) dT_L} \quad (\text{B7})$$

By straightforward calculation, we have

$$\eta_U^{\text{FT}}(\xi \rightarrow 0) = 1 - \frac{2\eta_C}{\eta_C - \ln(1 - \eta_C)}, \quad (\text{B8})$$

which can be re-expressed by $\eta_{\text{max}}(\xi \rightarrow 0)$ as

$$\eta_U^{\text{FT}}(\xi \rightarrow 0) = \frac{\eta_{\text{max}}(\xi \rightarrow 0)}{2 - \eta_{\text{max}}(\xi \rightarrow 0)} \quad (\text{B9})$$

This is the upper bound for $\xi \rightarrow 0$ we illustrated in Eq. (38). On the other hand, for $\gamma \rightarrow 0$, Eq. (32) becomes, by replacing $\eta_+(t)$ with $\eta_-(t) = \eta_C(t)/2$

$$\eta = \frac{\int_0^{t_f} \frac{\eta_C(t)}{2} T_H dS_{\text{re}}}{\int_0^{t_f} T_H dS_{\text{re}}} \quad (\text{B10})$$

$$= \frac{\int_{T_L}^{T_H} \frac{\eta_C(t)}{2} T_H \left[\frac{2-2\eta_C(t)}{2-\eta_C(t)} \right] \left(\frac{C_L dT_L}{T_L} \right)}{\int_{T_L}^{T_H} T_H \left[\frac{2-2\eta_C(t)}{2-\eta_C(t)} \right] \left(\frac{C_L dT_L}{T_L} \right)} \quad (\text{B11})$$

$$= \frac{\int_{T_L}^{T_H} \frac{T_H - T_L}{T_H + T_L} dT_L}{2 \int_{T_L}^{T_H} \frac{1}{T_H + T_L} dT_L}, \quad (\text{B12})$$

where we have used

$$\Delta Q_H^{(i)} = T_H^{(i)} \Delta S_{\text{re}}^{(i)} \quad (\text{B13})$$

and

$$\Delta Q_C^{(i)} = T_C^{(i)} \Delta S_{\text{re}}^{(i)} \left(\frac{2 - \eta_C^{(i)}}{2 - 2\eta_C^{(i)}} \right), \quad (\text{B14})$$

in the limit of $\gamma \rightarrow 0$. Finish the integral of Eq. (B12), we obtain

$$\eta_L^{\text{FT}} (\xi \rightarrow 0) = 1 + \frac{\eta_C}{2} \ln^{-1} \left(1 - \frac{\eta_C}{2} \right), \quad (\text{B15})$$

which is the lower bound η^{FT} of in the limit of $\xi \rightarrow 0$ as illustrated in Eq. (38).